Spatial variability of microbial communities and salt distributions across a latitudinal aridity gradient after heavy rains in the Atacama Desert

Jianxun Shen [1,*], Adam J. Wyness [2,3], Mark W. Claire [1], Aubrey L. Zerkle [1]

[1] School of Earth and Environmental Sciences and Centre for Exoplanet Science, University of St Andrews, St Andrews KY16 9AL, UK

[2] Sediment Ecology Research Group, Scottish Oceans Institute, School of Biology, University of St Andrews, St Andrews KY16 8LB, UK

[3] Coastal Research Group, Department of Zoology and Entomology, Rhodes University, Grahamstown 6139, South Africa

* Correspondence: js365@st-andrews.ac.uk

Abstract

Over the past 150 million years, the Chilean Atacama Desert has been transformed into one of the most inhospitable landscapes by geophysical changes, which makes it an ideal Mars analog that has been explored for decades. However, two heavy rainfalls that occurred in the Atacama in 2015 and 2017 provide a unique opportunity to study the response of resident extremophiles to rapid environmental change associated with excessive water and salt shock. Here we combine mineral/ salt composition measurements, amendment cell culture experiments, and next-generation sequencing analyses to study the variations in salts and microbial communities along a latitudinal aridity gradient of the Atacama Desert. In addition, we examine the reshuffling of Atacama microbiomes after the two rainfall events by comparing with previous researches. Analysis of microbial community composition revealed that soils within the southern arid desert were consistently dominated by Actinobacteria, Proteobacteria, Acidobacteria, Planctomycetes, Chloroflexi, Bacteroidetes, Gemmatimonadetes, and Verrucomicrobia. Intriguingly, the hyperarid microbial consortia exhibited a similar pattern to the more southern desert. Salts at the shallow subsurface were dissolved and leached down to a deeper layer, challenging indigenous microorganisms with the increasing osmotic stress. Microbial viability was found to change with aridity and rainfall events. This study sheds light on the structure of xerophilic, halophilic, and radioresistant microbiomes from the hyperarid northern desert to the less arid southern transition region, as well as their response to changes in water availability. Our findings may infer similar events that happened on the wetter early Mars.

Keywords: Atacama microbiome; function prediction; extremophiles; osmotic stress; salt amendments

1. Introduction

The Atacama Desert in northern Chile is the driest non-polar terrestrial desert on Earth, spanning more than 1,000 km in length from central Chile to southern Peru [1]. It is widely accepted as a Mars analog system based on its similar geomorphic landscape to Mars and multiple physicochemical aspects such as its hyperaridity, absence of water weathering, high ultraviolet (UV) radiation, low levels of organic carbon, and large reservoirs of oxidants [2]. The microbial life is unique from other terrestrial locations because these organisms have been exposed to extreme conditions since the late Jurassic 150 million years ago [1]. Thus, the environmental gradients within the Atacama Desert serve as an excellent model to investigate the influence of long-term aridity and different frequencies of precipitation-led water stress on soil microbial communities.

The newly available Atacama Database of microbiology [3] records 2,302 microorganisms in the Atacama Desert, with reference to 633 previously published papers between 1966 and 2016. Among these microorganisms, 1,741 species are from the Domain Bacteria. However, bacteria from unknown

phyla still comprise 40% of the currently recorded Atacama microbiome [3]. These microbes are distributed throughout the soil profile, with surface inhabitants are generally more tolerant to strong UV radiation, and those found deeper in soils are more tolerant to hypersaline conditions [4]. Despite the extreme aridity, desiccation may not be the sole or even the primary factor influencing microbial life in desert environments, and highly saline and oxidizing soils can also be crucial factors.

Counter-intuitively, an abrupt increase in water availability in hyperarid soils is extremely harmful to xerophilic microorganisms because these cells are induced to transform from the defensive or dormant state to the metabolically active state while unexpectedly being exposed to attack from extreme temperature and UV radiation [5]. In addition, excessive water causes high osmotic shock to the microbial semipermeable membrane and disturbs their survival strategies adapted for limited moisture [6,7]. After the heavy rainfall event in 2017 at the core region of the Atacama Desert, 75-87% of pre-rainfall species were undetectable, and no viable archaea or eukaryotes were detected in undrained brines [6]. Although these rainfall events can severely damage the extremotolerant microbial communities, previous studies demonstrated that the community structure can recover after one month in the central Namib Desert [8], or for more than one year at Salar Grande in the northern Atacama Desert [9], using a variety of biochemical mechanisms and osmoregulatory systems. Immediately after rainfall, microorganisms start producing proteins and metabolites that are crucial in fundamental biosynthetic pathways, energy supplements, desiccation resistance, radiation protection, and oxidation defense for the preparation of the upcoming hyperarid period [10].

Mars is likely to have been a much wetter planet around 4 billion years ago. Between then and the drier planet we recognize today, a transitional dry period with occasional moisture may have occurred [11]. Detection results by the Curiosity rover show evidence of temporary subsurface liquid during night-time on equatorial Mars and possibly beyond [12]. Therefore, the rare heavy rains in the hyperarid Atacama act as an analog to the transient availability of liquid water on Mars. This study investigated the differences in microbiome and soil salt compositions along a latitudinal precipitation gradient of the Atacama Desert after heavy rainfall events. Based on the soil relative humidity, Azua-Bustos et al. (2015) argued that María Elena South (MES) was drier than the commonly known hyperarid Yungay region [13], but no next-generation sequencing has been conducted to examine the MES microbial community. Thus, the research goals of this study are (1) to explore the microbial community structure and functions in MES and their changes toward the more humid sites, (2) to compare with some previous pre-rainfall Atacama Desert studies, and (3) to investigate how water and salt amendments affect microbial growth in Atacama soils.

2. Methods

2.1. Site descriptions and soil characterizations

Samples were collected from the Atacama Desert, northern Chile, in 2017 after two unprecedented heavy rainfall events that expanded from the Yungay region during March 24-26 in 2015 [4] and June 6-7 in 2017 [6] with 38.6 mm and 19.6 mm of rainfall respectively, according to the record at Antofagasta Rain Gauge (23.5975°S, 70.3867°W, Altitude: 50 m). The rainfall at each sampled site was listed in Table S1. Soils were collected from seven field sites along a ~800 km north to south latitudinal transect from 22°S to 29°S (Figure 1a and Table S1) as described in Shen et al. (2019). Briefly, samples were obtained from three hyperarid sites (María Elena South (MES), Point of No Return (PONR), and Yungay) and four transition zone sites (TZ-0, TZ-4, TZ-5, and TZ-6). Visible vegetation cover (sparse dried grasses and shrubs) appeared in regions close to the sampling sites of TZ-4, TZ-5, and TZ-6. Within each site, three random pits were sampled at a depth of 10-20 cm for geochemical analyses and DNA extractions, and the third sampling pit was additionally sampled for microbial cultivations. All samples were collected with a sterile sampling trowel, placed into sterile Whirl-Pak® bags (Nasco, Fort Atkinson, USA). Soils obtained in 2017 were collectively referred as AT-17.

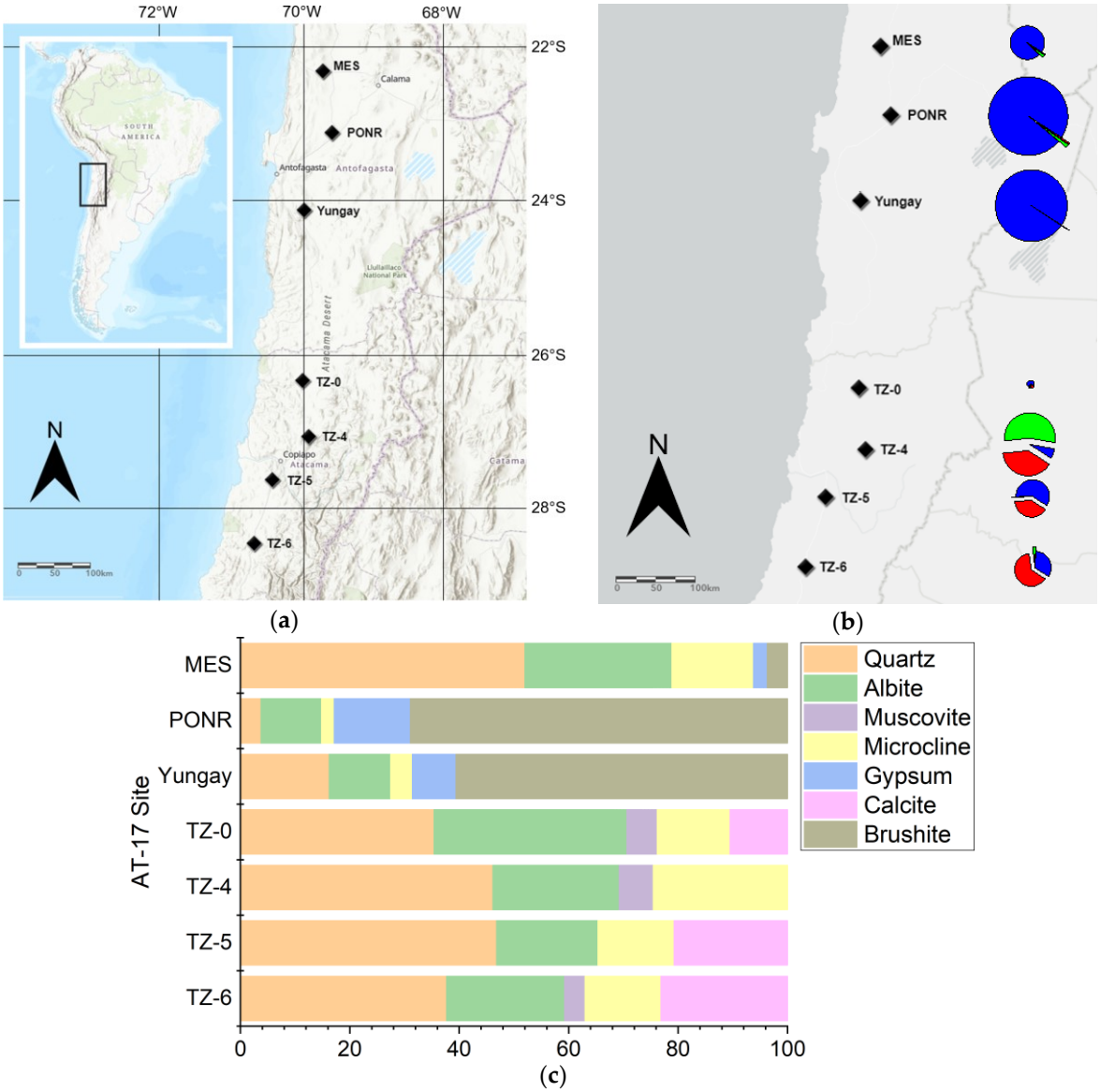

Figure 1. (**a**) Geographic locations of the Atacama Desert AT-17 sampling sites, including María Elena South (MES), PONR (Point of No Return), Yungay, Transition Zone 0 (TZ-0), TZ-4, TZ-5, and TZ-6. (**b**) Soil collection sites in the Atacama Desert, illustrating the major salt distribution of different sites. Size of pie charts represents the concentrations of soluble salts (Cl^-, red; NO_3^-, green; SO_4^{2-}, blue). The areas of pie charts range from 30 ppm to 17,000 ppm. (**c**) Percentages of different minerals in AT-17 samples determined by X-ray diffraction (XRD).

General soil properties (pH, electrical conductivity, major sediment elements by X-ray fluorescence (XRF) methods, and the concentrations of total organic carbon (TOC), total organic nitrogen (TON), carbonate, and nitrate) of AT-17 geochemical samples were reported in Shen et al. (2019). AT-17 geochemical samples were sieved through 1.4 mm prior to ion chromatography for soluble anion determinations as described in Shen et al. (2019).

Additionally, AT-17 soil samples for X-ray diffraction (XRD) were crushed using a Planetary Micro Mill (PULVERISETTE 6, FRITSCH) and sieved through a 355-μm sieve. The mineralogy of these crushed and sieved samples was analyzed on a Philips X-Ray Diffractometer (PW1830 generator, PW1050/80 goniometer, PW1710 diffractometer) using Co Kα radiation. Generator settings for the measurement were 30 kV, 30 mA, 3-70° range 2θ scan, 0.01° step, 1 s/step. Mineral phases were identified using the EVA 2 software from SOCABIM with the ICDD PDF-2 database.

2.2. DNA extractions and sequencing

Due to the low biomass in Atacama soils, AT-17 microbiological samples for DNA extraction were stored for one year at 4°C prior to finding a suitable cell lysis device, the Precellys 24 tissue homogenizer. The annual temperature of the Atacama Desert was between -5°C and 40°C [14,15], so we attempted to store soils at a low but comparable temperature to keep microbial communities alive but as dormant as possible. Due to the extreme aridness of these dry sandy soil samples, the effect of the storage duration should be insignificant, as even biolipids could preserve for more than one billion years [16]. DNA of AT-17 soils from three pits of each site were extracted together with an extraction blank using the MP Biomedicals™ FastDNA™ SPIN Kit for Soil following a modified manufacturer's protocol: during the cell lysis step, mixtures were incubated at room temperature for 1 hour. DNA extracts were amplified in triplicate for barcoded Illumina 16S metagenomic sequencing using KAPA HiFi HotStart ReadyMix (KAPA Biosystems, Roche, UK) and 16S rRNA primer pair 341F, 5'-CCTACGGGNGGCWGCAG-3', and 785R, 5'-GACTACHVGGGTATCTAATCC-3' using the Nextera index kit (Illumina®). Amplicons were quantified using an Invitrogen™ Qubit™ 3.0 Fluorometer, and only samples with enough yields (i.e., 3 pits in MES, 2 pits in TZ-0, 3 pits in TZ-4, 3 pits in TZ-5, and 3 pits in TZ-6) were passed for following preparation of sequencing. Triplicate amplicons from each pit were pooled together and concentrated by heating at 50°C to a final volume of 50 µl. 16S rRNA amplicons for Illumina MiSeq System was replicated and sequenced by following *16S Metagenomic Sequencing Library Preparation* together with a 20% PhiX control and the extraction blank using paired-end 300 bp reads with v3 Chemistry, modified by extending the amplicon PCR reactions from 25 to 29 cycles due to low product yield.

2.3. Assessments of bacterial abundance and viability

The abundance and viability of AT-17 microbial communities were analyzed via duplicate trypan blue staining assay within one month of sample collection, and cultivation methods within one month and replicate within half a year after sample collection. Duplicate AT-17 microbiological soils were suspended and 10× serially diluted two to four times to clear out any sand particles. 0.4% Trypan blue was added to 9× of the dilute solution. Viable (non-colored) and non-viable (blue) microbial cells were mounted on a Hirschmann Instruments™ Counting Chamber and counted using oil immersion light microscopy (AmScope). Detailed microbial cultivations of AT-17 samples were elucidated in Shen et al. (2019). Briefly, duplicate AT-17 samples from each site were suspended and homogenized in 1× volume of sterilized ultrapure water for microbial cultivations. Based on some preliminary tests for countable colony number estimations, an appropriate amount of soil suspension was spread on four types of culture medium: ultrapure agarose plate, tryptic soy agar plate, Luria-Bertani (LB) agar plate, and plate count agar. Visible colonies were counted after 20 days of incubation at 21°C.

2.4. Salt and water amendments

To inspect the effects of a variety of excessive dissolved salts on the viable microbial community, soils from each site were amended with 4.5 mL salt solutions. Solutions of 10% sodium chloride, 10% sodium sulfate, 10% sodium carbonate, 10% sodium acetate, and 10% sodium L-lactate were prepared in ultrapure water and autoclaved at 121°C for 30 min. After cooling to room temperature, 10 g of AT-17 soil was combined with the salt solution for 4 days at 21°C [17]. Duplicate salt-amended soils were suspended in appropriate volume of sterile ultrapure water and spread on ultrapure agarose, tryptic soy agar, LB agar, and plate count agar plates. Plates were sealed with Bemis™ Parafilm™ M Laboratory Wrapping Film and incubated for 20 days at 21°C prior to cell counting [18]. Colony forming units (CFUs) were determined by the multiplication of the number of colonies, dilution factor, and 1.45 to account for the addition of 4.5 mL solution to 10 g soil.

In addition, 4.5 mL, 3 mL, and 1.5 mL of sterile ultrapure water was added to each 10 g of AT-17 microbiological samples, which covers about the 1/3, 2/3, and full of soil area, respectively. Since the bottom diameter of Petri dishes used for culturing experiments is 90 mm, these volumes of water are equivalent to approximately 0.24, 0.47, and 0.71 mm daily precipitation, respectively. CFUs were

cultured and determined in the same manner as salt amendments. CFUs from cultivation experiments were converted via common logarithmic transformation. CFUs on salt amendments were standardized by subtracting their respective 4.5-mL water amendment groups; and CFUs on water amendments were standardized by subtracting their corresponding groups without any amendments.

2.5. Data analyses

Illumina sequence reads of AT-17 bacterial sequencing results were pre-processed with the open source package Quantitative Insights into Microbial Ecology 2 (QIIME 2). Reads were combined and demultiplexed into Casava 1.8 paired-end format. Reads of low quality were denoised with DADA2. Reads were filtered by trimming the first 13 base pairs and removing those of low quality, with ambiguous characters and missing barcoded primers, of a length less than 300 base pairs. AT-17 sequences were clustered into operational taxonomic units (OTUs) at a 99% similarity cutoff. The quality of total clustered sequences was double confirmed via noise and chimera pattern checking by VSEARCH and UCHIME. The representative taxonomic identities were aligned at 99% full-length sequence homology using pre-trained naïve Bayes classifier based on SILVA 132 marker gene reference database.

OTU tables were rarefied to remove sampling depth heterogeneity at 23,384 even sampling depth. Alpha diversity indices (binary logarithmic Shannon diversity, Faith's phylogenetic diversity, Pielou's Evenness, and observed OTUs) were computed with the alpha-phylogenetic package of QIIME 2. Alpha rarefaction curves were generated at the maximum 20,000 sequencing depth. Characteristic bacterial phyla associated with the sampling year and aridity were predicted and clustered with the q2-sample-classifier package showing the 100 most representative sequences. Analysis of composition of microbiomes (ANCOM) was employed to determine the genera that were significantly different among sampling year and aridity. Hierarchical clustering of each individual site using Bray-Curtis distance matrix was performed in Past 4.03.

Enzyme prediction and functional annotation of constructed sequences were performed in software Phylogenetic Investigation of Communities by Reconstruction of Unobserved States 2 (PICRUSt2) based on marker gene sequences. Amplicon sequence variants with nearest-sequenced taxon index more than 2 were excluded from the output. The abundance of predicted functional pathways was standardized as the percentage of the sum of read depths. MetaCyc pathway identifiers were linked to their respective functions at the secondary superclass level using the MetaCyc pathway hierarchy system.

3. Results

3.1. Soil geochemical features

To investigate the Atacama soil physicochemical context, samples were analyzed by total organic C and N (TOC and TON) quantifications, X-ray diffraction (XRD), X-ray fluorescence (XRF), and ion chromatography (IC). AT-17 sites were generally characterized by quartz (44±6%), albite (25±6%), and microcline (16±4%). However hydrated minerals, brushite and gypsum, took over a significant percentage (65±4% and 11±3% respectively) in the two post-rainfall hyperarid sites – PONR and Yungay (Figure 1c and Figure S1). The AT-17 soluble salts (i.e., chloride, nitrate, and sulfate) varied significantly between samples: chloride concentrations ranged from 5.8 parts per million (ppm) in TZ-0 to 3,600 ppm in TZ-4; nitrate ranged from 1.9 ppm in TZ-0 to 5,000 ppm in TZ-4; and sulfate ranged from 24 ppm in TZ-0 to 17,000 ppm in PONR (Table S2). Total soluble salts remained at about the same level within PONR and Yungay and within MES, TZ-5, and TZ-6 (Figure 1b).

3.2. Bacterial abundance and viability

To assess the abundance and viability of bacterial communities, trypan blue staining assay and cell culture experiments were employed. Trypan blue staining-determined viable and total cell counts of

hyperarid sites PONR and Yungay were noticeably lower than the southern transition sites (Figure 2a and Table S3). However, no significant difference in the viable and total cell counts was noted between the northernmost hyperarid site MES and southern transition sites. The active culturable colonies on different types of culture plates increased appreciably toward the transition zone with higher annual precipitation (Figure 2b, c, d, e). In general, TZ-5 had lower microbial abundance than TZ-4 and TZ-6. The viable : non-viable ratios in AT-17 soils varied from 0.7 in TZ-5 to 8.0 in MES (Table S3), and these ratios were generally higher in the dryer sites than the more humid sites.

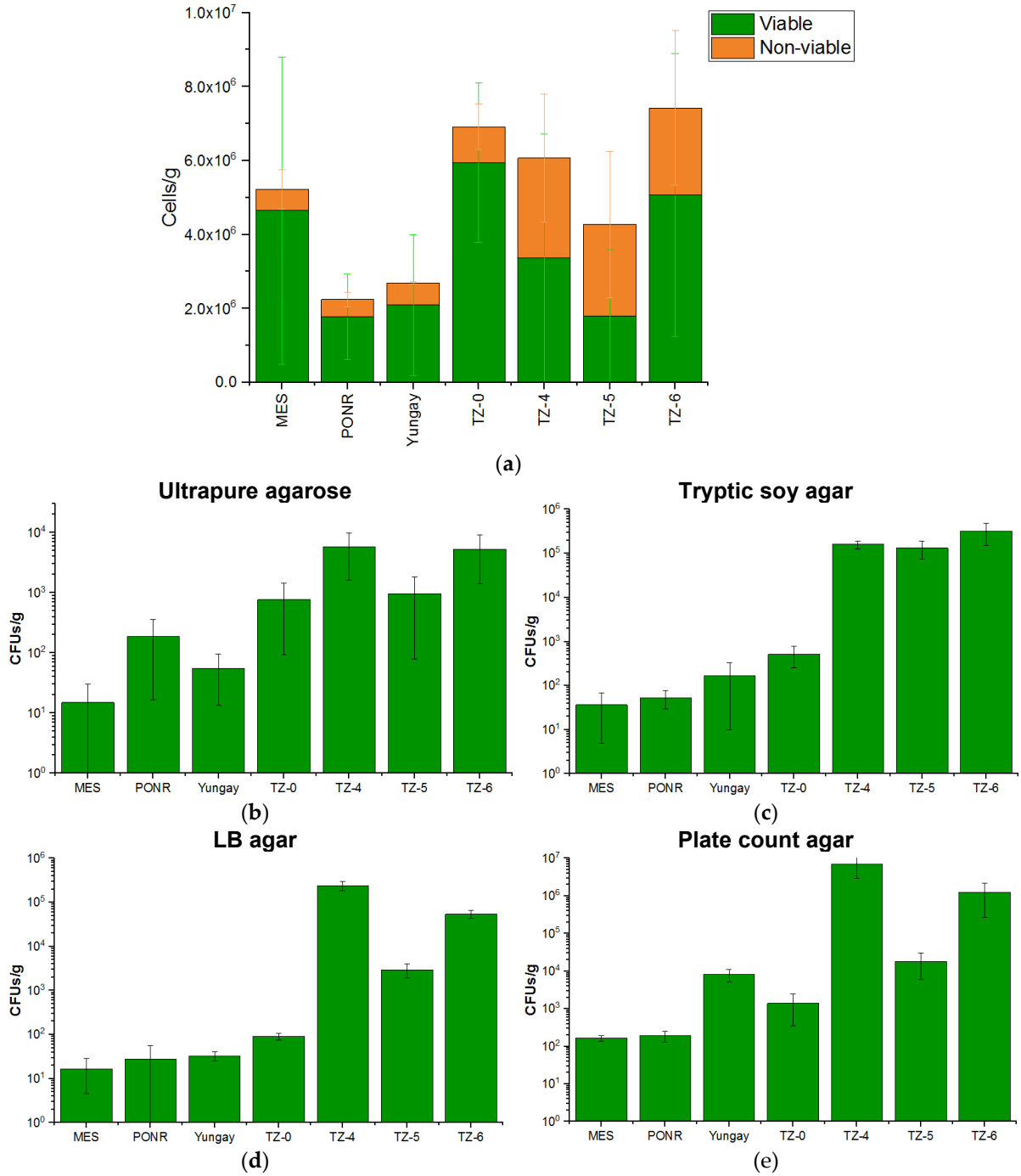

Figure 2. (**a**) Cumulative bacterial cell counts per gram of soils of AT-17 samples determined by trypan blue staining assay analyses. And viable aerobic heterotrophic colony forming units (CFUs) on (**b**) ultrapure agarose, (**c**) tryptic soy agar, (**d**) LB agar, and (**e**) plate count agar plates.

Within the hyperarid core of the Atacama Desert in 2017, TOC was negatively correlated with the contents of sediment sodium (Na_2O) and chloride (Cl) (Figure 3a and b). However, TOC was positively

associated with the concentrations of the water-soluble chloride (Cl) and sulfate (SO_4) (Figure 3c and d).

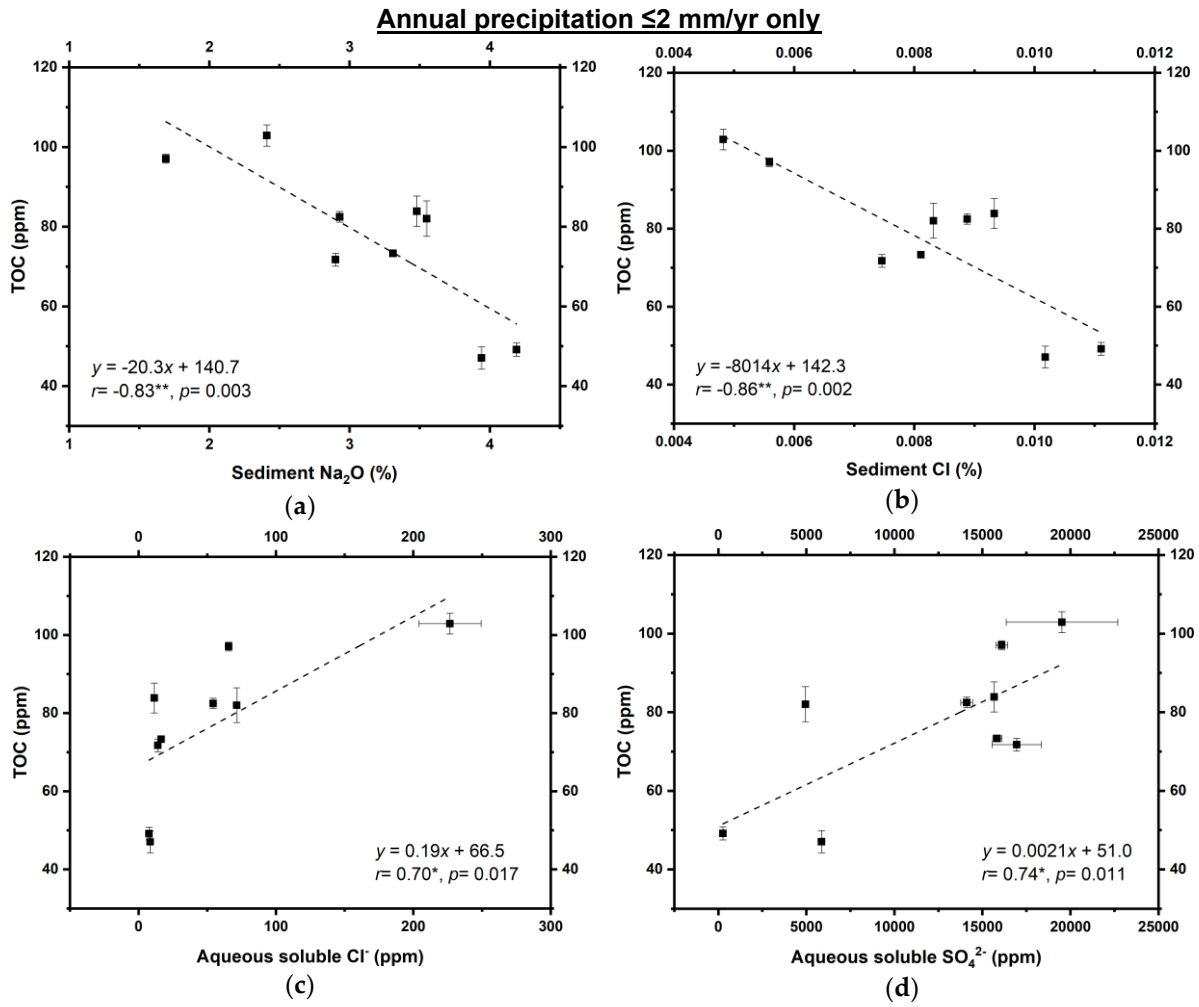

Figure 3. Plots of total organic carbon (TOC) and (**a**) sediment sodium, (**b**) sediment chloride, (**c**) water soluble chloride, and (**d**) water soluble sulfate in hyperarid sites.

Soil microbial communities showed different preferences to the water volume on different agar plates. Water amendment cultures (1.5, 3 and 4.5 mL) demonstrated that transition sites were slightly less water-limited than hyperarid sites because increasing water content did not change CFUs (Table 1 and Table S4). In general, an increase in water content from 0 mL to 4.5 mL increased bacterial cell counts, but the growth rates did not always increase with further water addition. No CFU decrease in the water amendments was more than 1.5 orders of magnitude (Table 1). Overall, excessive sodium chloride and sodium carbonate amendments decreased cell counts; sodium sulfate and sodium acetate had no effect; and sodium L-lactate increased cell counts (Table 2 and Table S4). Sites with higher annual precipitation generally had a higher tolerance or higher preference to the amendments with these salts, except for sodium carbonate (Table 2).

Table 1. Results of cell cultures on ultrapure agarose, tryptic soy agar, LB agar, and plate count agar plates with water amendments, recording the change in the order of magnitude of CFUs with water amendments (all numbers are scaled by logarithmic transformation and normalized as the difference from the plates without amendments). Positive effects of different volumes of water on microbial growth are bolded, and those caused increase in CFUs more than 1 and 2 orders of magnitude are labeled with $^{+}$ and $^{++}$, respectively.

Type of culture plate	Amendment	MES	PONR	Yungay	TZ-0	TZ-4	TZ-5	TZ-6
Ultrapure agarose	1.5 mL H_2O	-1.18	**0.05**	**0.55**	-0.89	-0.32	-1.15	-1.08
	3 mL H_2O	-1.18	**0.41**	**0.39**	-0.60	-0.27	-0.97	-0.63
	4.5 mL H_2O	-1.18	-1.11	**0.29**	-0.84	-0.21	-1.05	-0.90
Tryptic soy agar	1.5 mL H_2O	**1.15**$^{+}$	**0.42**	-0.58	-0.24	-0.17	-0.36	-0.16
	3 mL H_2O	**0.05**	-0.19	**1.57**$^{+}$	-0.25	-0.30	-0.05	**0.13**
	4.5 mL H_2O	**2.20**$^{++}$	**1.80**$^{+}$	**1.83**$^{+}$	-0.22	**1.01**$^{+}$	-0.41	**0.20**
LB agar	1.5 mL H_2O	**0.63**	**0.29**	-0.41	**0.19**	-1.47	-0.21	**0.49**
	3 mL H_2O	**0.34**	**0.53**	**2.36**$^{++}$	**0.42**	-0.95	**0.22**	**0.32**
	4.5 mL H_2O	-0.36	**2.46**$^{++}$	**2.06**$^{++}$	**0.73**	**0.71**	-0.40	**0.45**
Plate count agar	1.5 mL H_2O	**0.65**	**1.65**$^{+}$	**0.02**	-0.65	-0.33	**0.51**	**0.71**
	3 mL H_2O	**1.10**$^{+}$	**0.13**	**0.75**	-0.76	-0.41	**0.16**	-0.32
	4.5 mL H_2O	**0.91**	**2.65**$^{++}$	**0.94**	-0.34	**0.29**	**0.84**	**0.52**

Table 2. Results of cell cultures on ultrapure agarose, tryptic soy agar, LB agar, and plate count agar plates with salt amendments, recording the change in the order of magnitude of CFUs with salt amendments (all numbers are scaled by logarithmic transformation and normalized as the difference from the plates with 4.5-mL water amendments). Negative effects of different salts on microbial growth are underlined, and those caused the decrease in CFUs more than 1, 2, 3, and 4 orders of magnitude are labeled with $^{-}$, $^{--}$, $^{---}$, and $^{----}$, respectively.

Type of culture plate	Amendment	MES	PONR	Yungay	TZ-0	TZ-4	TZ-5	TZ-6
Ultrapure agarose	Chloride	0	-0.78	0.64	0.42	-0.04	1.67	0.64
	Sulfate	0	-1.16^{-}	-1.64^{-}	-0.62	-0.35	0	0.06
	Carbonate	0	-0.48	-0.01	-2.05^{--}	-0.48	0	0.72
	Acetate	0	-1.16^{-}	0.37	0.64	-0.94	0.90	0.35
	L-lactate	2.34	1.87	0.67	1.00	-1.49^{-}	1.63	0.18
Tryptic soy agar	Chloride	-2.90^{--}	-2.45^{--}	0.50	-0.24	-1.59^{-}	1.22	0.01
	Sulfate	-2.42^{--}	-2.85^{--}	0.05	0.58	-0.77	0.82	0.01
	Carbonate	-1.16^{-}	-2.54^{--}	0.38	-1.63^{-}	-3.74^{---}	0.02	-0.14
	Acetate	-3.38^{---}	-3.15^{---}	-2.09^{--}	-0.07	-0.51	0.44	0.34
	L-lactate	0.58	-1.77^{-}	-0.21	0.27	0.03	0.20	-0.03
LB agar	Chloride	-0.86	-3.52^{---}	-1.23^{-}	-0.56	-2.61^{--}	-0.08	-0.11
	Sulfate	0.48	-3.52^{---}	-1.41^{-}	0.24	-2.12^{--}	0.40	0.38
	Carbonate	2.57	-2.74^{--}	-1.84^{-}	-2.69^{--}	-3.60^{---}	0.22	-1.54^{-}
	Acetate	0.12	-3.22^{---}	-1.18^{-}	-0.14	-0.35	0.57	0.59
	L-lactate	1.35	-1.64^{-}	0.47	0.34	0.43	0.72	0.44
Plate count agar	Chloride	-2.75^{--}	-3.21^{---}	-3.38^{---}	-0.43	-0.85	-0.33	-0.86
	Sulfate	-1.16^{-}	-1.99^{-}	-4.84^{----}	1.16	-0.34	-0.33	-0.99
	Carbonate	0.07	-2.69^{--}	-2.60^{--}	-1.08^{-}	-3.49^{---}	-0.29	-1.37^{-}
	Acetate	-2.75^{--}	-3.65^{---}	-2.71^{--}	-0.52	-0.70	-0.73	-0.49
	L-lactate	0.33	-2.46^{--}	-0.01	0.65	0.32	0.50	-0.20

3.3. Microbial community diversity and pathway analysis

To investigate the impact of aridity on Atacama microbial communities, we performed a soil metagenomic analysis of AT-17 bacterial sequence data. Unfortunately, since the DNA concentrations extracted from PONR and Yungay were not sufficient for sequencing, we could not compare them. For the remaining samples, biodiversity was the lowest in MES, while the highest in TZ-5 and TZ-6 (Table 3 and Figure S2). The diversity was slightly higher in TZ-0 than TZ-4.

Table 3. Shannon diversity, Faith's phylogenetic diversity (PD), species evenness, and observed OTU richness indices of AT-17 samples.

Site	Shannon (binary log)	Faith's PD	Evenness	Observed OTUs
AT17-M1 (MES pit 1)	6.73	25.3	0.833	272
AT17-M2 (MES pit 2)	5.59	16.8	0.767	156
AT17-M3 (MES pit 3)	5.60	18.9	0.772	152
AT17-T01 (TZ-0 pit 1)	7.59	43.9	0.799	722
AT17-T02 (TZ-0 pit 2)	6.99	37.6	0.767	550
AT17-T41 (TZ-4 pit 1)	7.09	38.6	0.793	494
AT17-T42 (TZ-4 pit 2)	7.11	38.4	0.787	522
AT17-T43 (TZ-4 pit 3)	6.72	33.1	0.788	371
AT17-T51 (TZ-5 pit 1)	8.43	50.6	0.892	699
AT17-T52 (TZ-5 pit 2)	8.49	73.6	0.833	1172
AT17-T53 (TZ-5 pit 3)	7.84	49.9	0.842	632
AT17-T61 (TZ-6 pit 1)	8.32	53.0	0.859	821
AT17-T62 (TZ-6 pit 2)	8.50	52.8	0.879	813
AT17-T63 (TZ-6 pit 3)	8.60	52.8	0.889	815

In total, 464 bacterial families, 832 genera, and 1,112 species were determined. Considering their large quantity, we plotted at the phylum level only. The bacterial phyla dominated soils within the AT-17 hyperarid MES were Actinobacteria (66.27±3.94%), Proteobacteria (12.65±2.31%), and Chloroflexi (11.83±0.79%); and those dominated soils within AT-17 arid southern desert were similarly Actinobacteria (50.42±11.84%), Chloroflexi (16.14±8.27%), and Proteobacteria (11.47±2.92%) (Figure 4a).

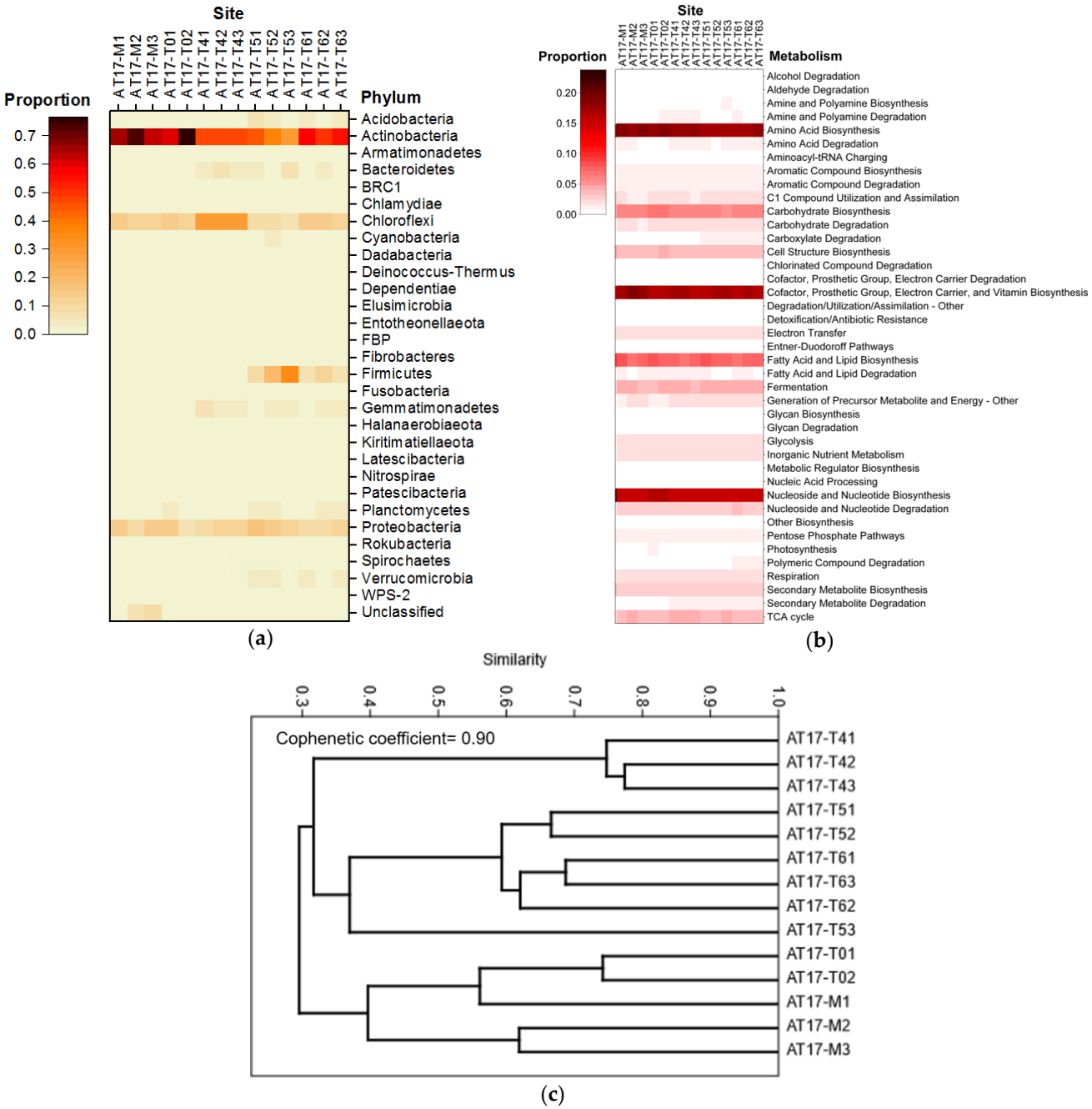

Figure 4. (**a**) The heatmap illustrating phylum level microbial composition in soils of the Atacama Desert from AT-17 sequencing data. (**b**) Relative abundance of microbial metabolisms presented as the secondary superclass in MetaCyc classification system. (**c**) Hierarchical clustering (Bray-Curtis distance matrix and unweighted pair group method with arithmetic mean algorithm) of microbial compositions at the species level in AT-17 sites. Abbreviations as in Table 3.

ANCOM results suggested that genus *Streptomyces* (Actinobacteria) was significantly different (W= 703, p< 0.05) between the hyperarid core and transition zone. Characteristic known genera in the hyperarid core were *Thermus* (Deinococcus-Thermus), *Escherichia-Shigella* (Gammaproteobacteria), and *Pseudomonas* (Gammaproteobacteria), while characteristic known genera in the transition zone were *Rubrobacter* (Actinobacteria), uncultured Gammaproteobacteria, *Bacillus* (Firmicutes), and *Solirubrobacter* (Actinobacteria).

Hierarchical clustering of species indicated that the three pits within each individual AT-17 site generally had 40%-75% similarity (Figure 4c). The hyperarid microbiome in MES was most similar to

the most northern transition site TZ-0, which is in agreement with the statistical classification based on soil fundamental physicochemical parameters [17].

Because of the microbiomic similarity, the metagenome function of MES microbiomes was comparable to the southern transition sites (Figure 4b). However, the hyperarid site MES had fewer proportions of amine and polyamine biosynthesis, aminoacyl-tRNA charging, detoxification, glycan biosynthesis and degradation, nucleoside and nucleotide degradation, polymeric compound degradation, and secondary metabolite degradation.

Various adaptation pathways coupled with environmental stress reactions (including regulations of desiccation, irradiation, salinity, and osmotic pressure) and salt/ small organic consumptions were predicted based on feature sequences (Figure S3). Compared to transition sites, MES had slightly lower proportions of pathways coupled with stress reactions, but higher proportions of nitrate and sulfate utilization pathways (Table 4).

Table 4. Percentages of metabolic pathways related to stressor responses from Atacama soils in the hyperarid core and the transition zone sampled in 2017.

Stressor response pathways (%)	Hyperarid AT-17	Transition AT-17
Desiccation/ dehydration	3.35	3.45
Ultraviolet/ irradiation	3.01	3.39
Salinity	1.40	1.25
Simple organic molecule metabolisms	8.37	9.18
Nitrate reduction/ assimilation	2.79	2.62
Sulfate reduction/ assimilation	1.25	1.15
Osmotic lysis	7.19	7.38

4. Discussion

4.1. Effects of water and salt regulations on microbial growth

In the Atacama Desert, atmospherically derived nitrate and other oxyanion salts accumulate in the soil [19], leading to variable soil conductivity, high oxidation potential, and abiotic chemical decomposition of soil organic matter. Our results indicated that while precipitation was a constraint for microbiomes, other geochemical properties also affected the microbial community structure, especially salt availability. As the aridity increased toward the northern hyperarid desert, soluble compounds accumulated at the surface and shallow subsurface. On the other hand, increased precipitation in the southern transition zone restricted these accruals as more salts were delivered deeper, but it also simultaneously enhanced soil salt availability [17,19].

We found that the viable and total cell counts were remarkably lower in PONR and Yungay, the two hyperarid sites that received massive rainfall before sampling, than the other sites (Figure 2a and Table S3). However, microbial viability in Atacama soils was variable, with the lowest in the southern desert sites TZ-4 to TZ-6, which was opposite to a previous study before the recent rainfall events [20]. This increased viability in the hyperarid region could be a consequence of the loss of non-viable cells as an additional implication of the rainfall discharge effects [21,22]. Across the AT-17 sampling transect, the percentage of viable microbial cells decreased from ≤ 89% in northern hyperarid soils to 39% in southern transitional soils (Table S3), similar to other extreme environments [23-25] and lower than typical soils usually with more than 90% viable cells [26,27].

The microbial cultivation experiments (without any amendments) demonstrated that the CFUs from AT-17 samples increased up to 4 orders of magnitude from the hyperarid sites to transition sites (Figure

2b, c, d, e and Table S4). The reasons for the difference between viable cell counts and culturable microbial colony numbers might be that (1) more unculturable species lived in the hyperarid core [28,29], and that (2) most of the hyperarid microbiomes were metabolically inactive [2,4,20,30]. Since the Actinobacteria-dominated microbial community structure did not alter much between the hyperarid AT-17 and transition AT-17 sites (Figure 4a), the latter hypothesis might play a more important role in the culturable CFUs. The agar cultured bacteria from surface samples collected within the Atacama Desert were limited in diversity, and the majority were members of Actinobacteria and Firmicutes. A small amount of Proteobacteria and Bacteroidetes has also been recovered [2,18]. More specifically, previously identified culturable bacteria belonged to *Geodermatophilaceae*, *Sphingomonas*, *Bacillus*, *Arthrobacter*, *Brevibacillus*, *Kocuria*, *Cellulomonas*, *Hymenobacter*, *Asticcacaulis*, *Mesorhizobium*, *Bradyrhizobium*, *Afipia*, *Alphaproteobacteria*, and *Betaproteobacteria* [31,32]. On our agar plates, these bacterial taxa acted as representatives of the whole microbial community from their sampled sites. Thus, the manner of growth and the change in CFUs of our cultivation experiments primarily reflected the preferences of bacteria within these taxa.

The water amendment experiments suggested that active culturable microorganisms were not impaired by rainfall that was less than 1 mm per day, as the volumes of water we added to these agar plates. Although the proliferation of some of these microbes manifested a decreasing trend after the abrupt water wash, more microbes benefited from the addition of water (Table 1 and Table S4). However, when precipitation reached as high as the two unprecedented rainfall events (38.6 mm and 19.6 mm, respectively) in a few days, massive water input could dissolve soluble salts and concentrated them down to more 20 cm depth [33,34]. Amendments with excessive dissolved sodium chloride and sodium carbonate inhibited the growth of active microorganisms on agar plates; amendments with excessive dissolved sodium sulfate and sodium acetate made no difference in microbial growth; only excessive sodium L-lactate amendments promoted the growth of active culturable microbes (Table 2 and Table S4). Unfortunately, since organic C salts were limited in the oxidizing natural environment of the Atacama Desert [2,35], the dissolved material and the extreme water addition might only harm the indigenous microbial communities [6,10], at least in the short term.

In comparison with the results of microbial cultures, the negative correlations between TOC (an approximation of all grain-bound biomass) [17,32,36] and sediment sodium/chloride within the hyperarid core (Figure 3a and b) were consistent with the negative effects of sodium chloride and some other sodium salts on microbial proliferation (Table 2 and Table S4) [18]. However, TOC content in the hyperarid core was positively associated with water soluble chloride (Figure 3c). This inconsistency of the relationships between microbial biomass and chloride in different forms could be explained with several hypotheses. Firstly, some chloride minerals such as halite were highly hygroscopic. Secondly, the deliquescence process within chloride minerals provided moisture to endolithic microbial communities [37,38]. Finally, the soluble chloride concentration indicated the portion of chloride that deliquesced. The positive correlation between TOC and soluble chloride indirectly reflect the beneficial effect of salt deliquescence on microbial biomass, but not a benefit directly from chloride ions.

Furthermore, water soluble sulfate also contributed to microbial biomass as a long-term outcome (Figure 3d), which again disagreed with salt amendment experiments (Table 2 and Table S4). Since sulfate in the Atacama Desert was usually formed in hydrated forms such as gypsum (Figure 1c), more sulfate indicated that larger proportions of gypsum could potentially provide crystallization water to nearby microorganisms [39,40]. Additionally, some microorganisms could reduce sulfate for energy production and sulfur assimilation (Figure S3 and Table 4) [41,42]. Therefore, higher sulfate concentrations could both elevate the moisture in a microhabitat and supply nutrients for microbial life.

4.2. Microbial communities and metabolic functions along the latitudinal aridity gradient

After the two heavy rainfall events during 2015 and 2017, soluble salts at the shallow subsurface of soils were dissolved and transported to depth. For example, the proportions of brushite and gypsum which contain crystallized water molecules increased remarkably in PONR and Yungay where heavy rainfalls had the largest influence (Figure 1c and Figure S1) compared to minerals before rainfalls [43]; and chloride minerals became undetectable in all AT-17 sites. Adequate metagenome failed to be extracted from PONR and Yungay soils within the hyperarid area. These two sampling sites had undertaken the most amount of precipitation 6 months before our sampling. Despite more culturable colonies, the trypan blue assay-determined viable and total cell counts of PONR and Yungay were remarkably lower than the other sites, including MES. Additionally, Azua-Bustos et al. (2018) found that excessive rainfall input could significantly diminish microbial communities in Atacama [6]. Given the water amendment cell culture experiments in this study, water addition probably raises the growth rate of culturable species only. This result also indicated that the extracted metagenomic DNA was contributed more by unculturable extremophilic species.

Although the diversity of unknown phyla was high [3], the relative abundance of these species was usually very low (Figure 4a). Soils of the southern arid desert were generally homogeneous in microbial composition and dominated (>1%) by Actinobacteria, Chloroflexi, Proteobacteria, Firmicutes, Bacteroidetes, Gemmatimonadetes, Planctomycetes, Acidobacteria, and Verrucomicrobia (Figure 4a), phyla commonly detected in arid desert environments. MES of lower relative humidity than the hyperarid Yungay region [13] possessed 16% more Actinobacteria percentage than southern arid sites (Figure 4a). However, compared to Yungay, MES had higher microbial abundance (Figure 2a), which might result from proper but not overwhelming rainfall input. Given the 40% similarity between MES and TZ-0 species (Figure 4c), the structure of microbial communities in the hyperarid region largely shifted toward a pattern that is more common in the southern transition zone (Figure 4c), to one dominated by Actinobacteria, Proteobacteria, and Chloroflexi (Figure 4a). This shift indicated the occurrence of a water-driven microbial community perturbation and reorganization in the hyperarid core. As for metabolisms, MES microorganisms had lower proportions of degradation pathways of amines, polyamines, carboxylates, polymeric compounds, and secondary metabolites to save essential organic sources for survival (Figure 4b).

Pre-rainfall hyperarid soils were shown to be predominantly composed of Deinococcus-Thermus and Aquificae as previously reported in Shirey (2013), and other characteristic bacterial phyla included Acetothermia, Armatimonadetes, Hydrothermae, and Thermotogae, bacteria within which generally adapted to nutrient-depleted and high temperature conditions. Actinobacteria that lived in the pre-rainfall hyperarid core of the Atacama Desert before rainfalls were extremely low [20]. Besides the long-term hyperaridity, the deficiency of extractable Actinobacteria before rainfall may be also caused by incomplete extraction: some Actinobacteria such as its classes Actinobacteria, Acidimicrobiia, and Rubrobacteria could form spores that were difficult to break down during DNA extraction to counterattack ultraviolet radiation and dehydration [44]. Analogous to Actinobacteria, the decreased proportions of Firmicutes (majorly Bacilli, and minorly Clostridia, Erysipelotrichia, and Limnochordia) in the hyperarid core after heavy rainfalls might also be a result of their sporulation [45].

Deinococcus-Thermus bacteria, are well-known extremophiles that have previously been detected in calcites, halites, microbialites, and gypsum evaporites of the Atacama Desert. After heavy rains, within the phylum of Deinococcus-Thermus, dominance shifted from of the order Thermales [20], who were mostly thermoresistant, to a dominance of the order Deinococcales, who were both thermoresistant and radioresistant [46,47]. This shift might be triggered by the negative facet of water-driven microbial metabolic activation: since water revived dormant microbes, these microbes disarmed sporulation and confronted the harsh ambient conditions, especially ionizing irradiation [7,8]. Therefore, the Deinococcus-Thermus population shifted to a more Deinococcales-dominant structure.

On Mars, nocturnal availability of a thin layer of liquid water at the subsurface [12] can nourish indigenous Martian “microbes” and allow them to slowly thrive with a small amount of moisture daily

[7]. The cycle of desiccation and rewetting facilitates dead microbial decomposition, releasing intracellular organics and soil organic matters [8], which also remobilizes nutrients for live microorganisms that are activated from dormancy by liquid water. However, most microorganisms were not culturable (staying dormant or dead) when exposed to brine [6]. Thus, our findings suggested feasibly detectable Martian "life" might concentrate at the regions of temperate temperature, i.e., around the equatorial regions, and during the daytime after the evaporation of the film of liquid brine.

Availability of supporting data

The raw sequencing data for microbiome analyses of AT-17 samples in this study are available from the National Center for Biotechnology Information (NCBI) under BioProject ID PRJNA595740.

Funding

This research was funded by European Research Council (ERC) under the European Union's Horizon 2020 Research and Innovation Programme (Grant Agreement 678812) (to MWC) for 2017 sampling and various geochemical characterizations, and John Templeton Foundation (Grant Agreement 60501) (to AJW) for assistance with sequencing and bioinformatics. JS also acknowledges support from the China Scholarship Council (CSC).

Acknowledgments

We thank Matthew Holden in the School of Medicine, University of St Andrews, for generously providing the Illumina MiSeq sequencing system. We thank Kerry Pettigrew in the School of Medicine, University of St Andrews, for assisting with Qubit DNA quantitation. We thank Claire Cousins, Lotta Purkamo, and Mark Fox-Powell in the School of Earth and Environmental Sciences, University of St Andrews, for useful discussions upon microbiological analyses.

Conflict of Interest Statement

The authors declare that the research was conducted in the absence of any commercial or financial relationships that could be construed as a potential conflict of interest.

Supplementary materials

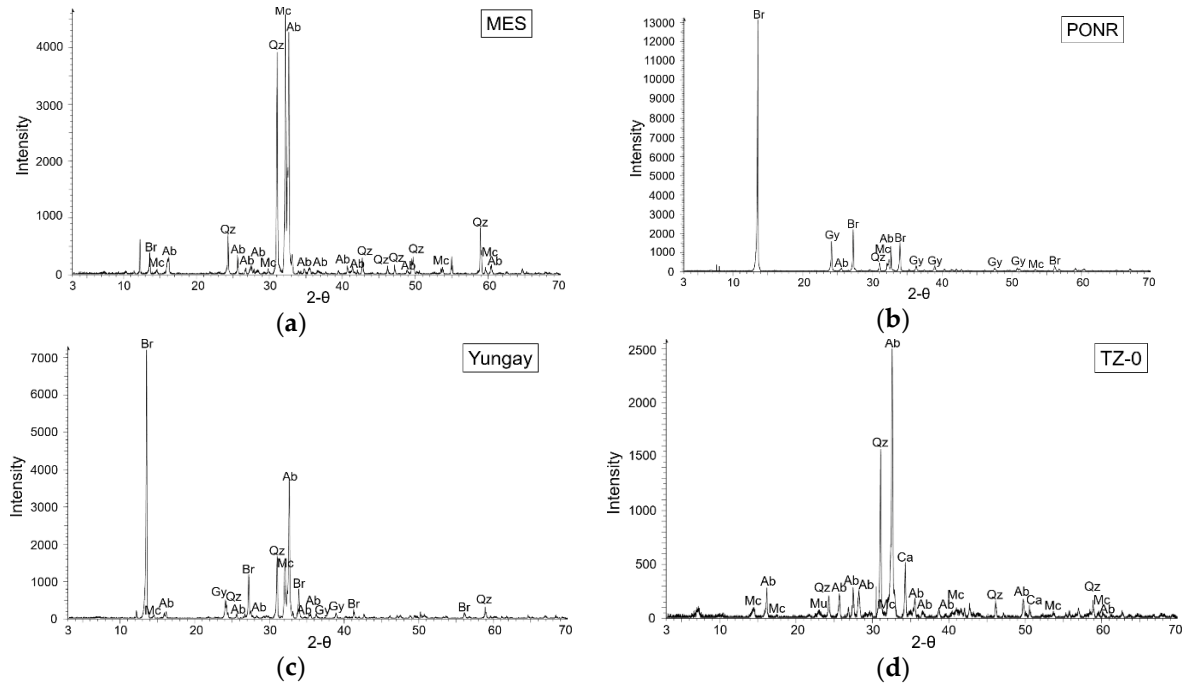

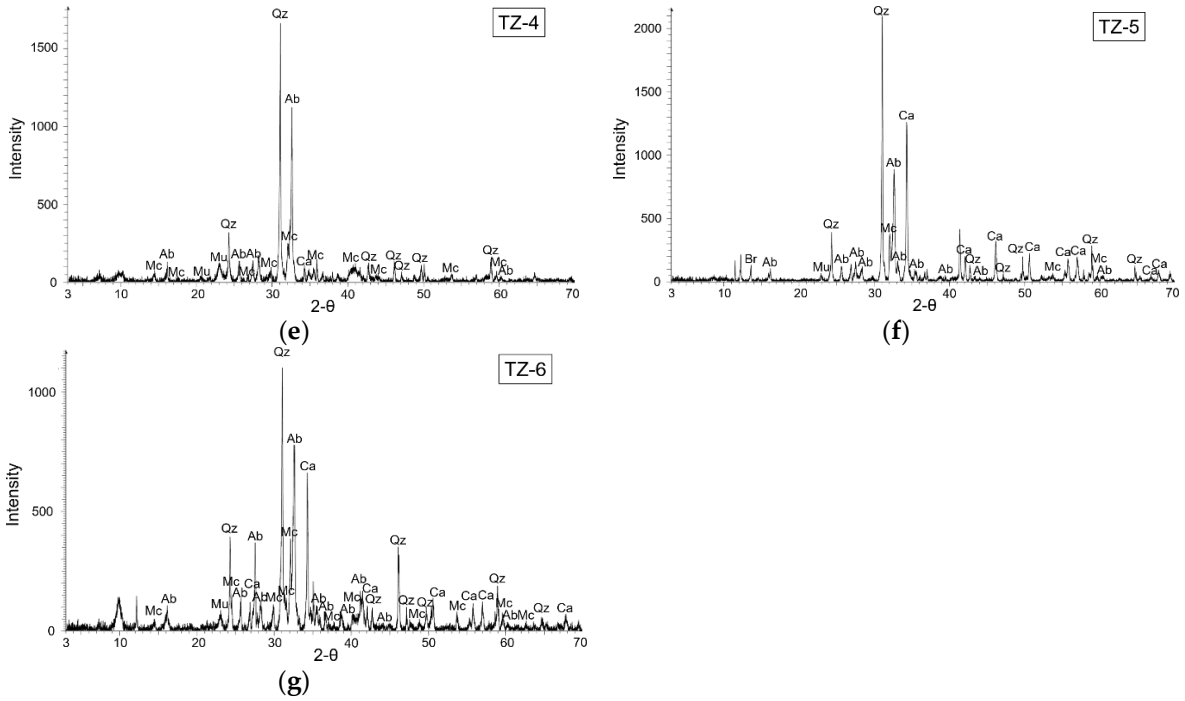

Figure S1. Mineral compositions of AT-17 soils determined X-ray diffraction (XRD) analysis. (Qz, quartz; Ab, albite; Br, brushite; Gy, gypsum; Mu, muscovite; Ca, calcite; Mc, microcline)

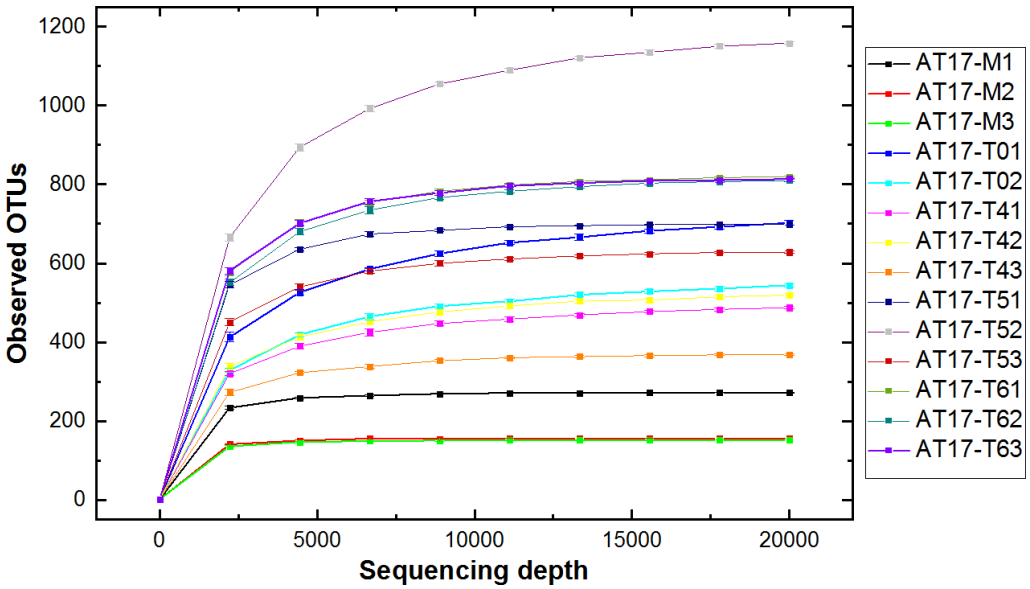

Figure S2. Observed OTUs richness as a function of the number of sequences per sample at 20,000 sampling depth. An OTU definition of sequence homology at or above 99%. Error bars of rarefaction analysis were shown. Abbreviations as in Table 3.

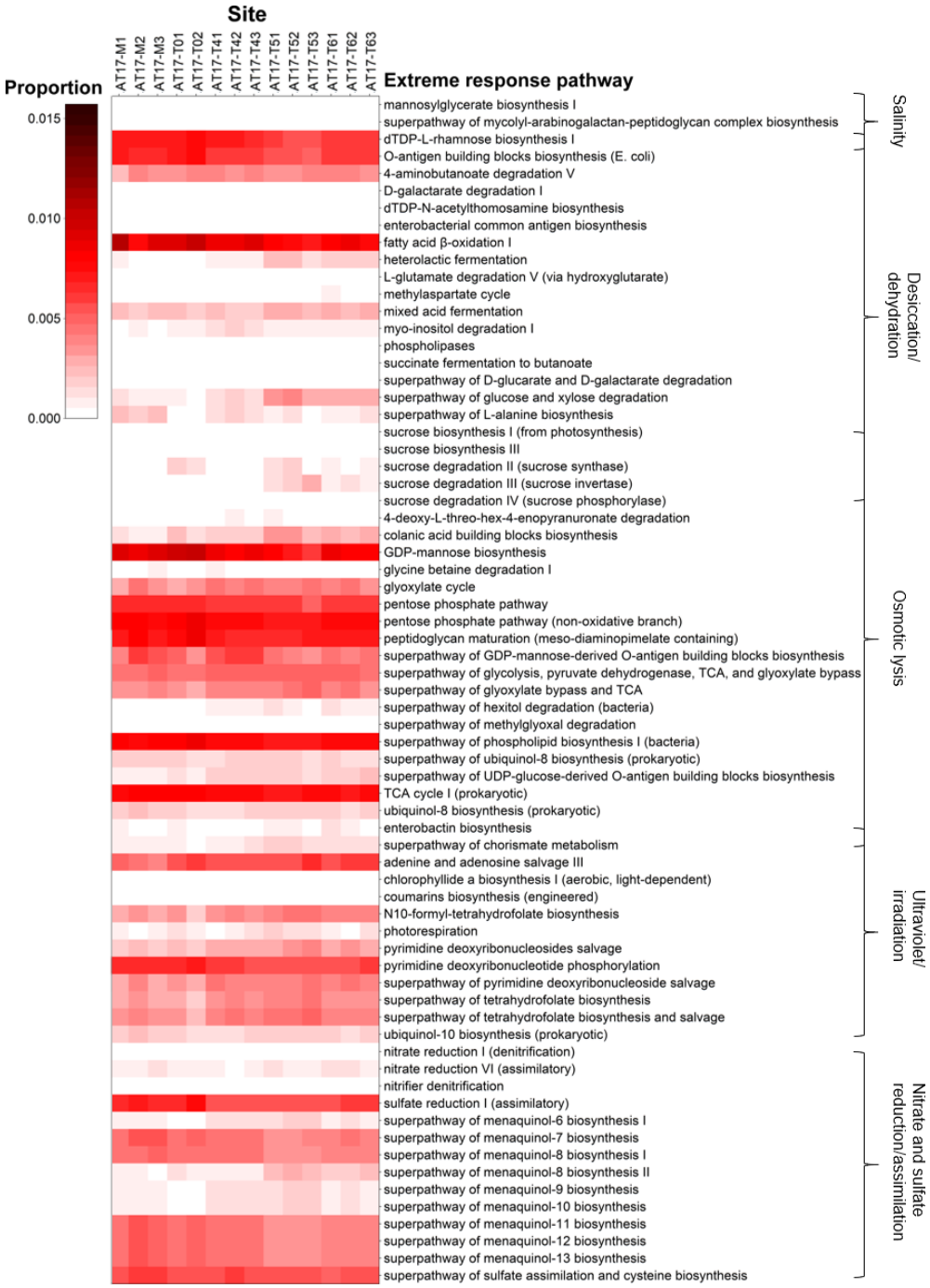

Figure S3. Relative abundance of microbial functional pathways that are associated with stressor responses from Atacama soil samples across a precipitation gradient collected in 2017.

Table S1. Geographic coordinates and altitudes of AT-17 sampling sites and the daily precipitation during the June 6-7 2017 heavy rainfall (modeled by https://www.ventusky.com/) [17,20].

Site	Latitude (°S)	Longitude (°W)	Altitude (m)	Precipitation (mm/day)
AT-17 MES	22.2641	69.7243	1493	3.3
AT-17 PONR	23.0726	69.5892	1493	10.1
AT-17 Yungay	24.0884	69.9945	1007	13.4
AT-17 TZ-0	26.3222	70.0128	1106	2.9
AT-17 TZ-4	27.0565	69.9228	1658	3.9
AT-17 TZ-5	27.6051	70.4458	588	0.4

AT-17 TZ-6	28.4100	70.7270	658	0.1

Table S2. Concentrations (means ± standard errors) of soluble chloride, nitrate, and sulfate in AT-17 samples.

Sample	Cl^- (ppm)	NO_3^- (ppm)	SO_4^{2-} (ppm)
MES pit 1	7.5±0.1	35.7±0.3	260.4±3.2
MES pit 2	71.4±1.2	238.4±3.6	4948.0±60.5
MES pit 3	8.5±0.1	52.1±0.2	5865.3±24.6
PONR pit 1	54.3±1.6	147.5±2.5	14108.4±333.1
PONR pit 2	226.7±22.6	362.0±39.1	19520.1±3172.1
PONR pit 3	65.5±2.0	157.7±2.6	16093.5±333.0
Yungay pit 1	16.4±0.9	23.8±0.1	15840.4±248.4
Yungay pit 2	14.0±0.2	19.3±1.0	16941.8±1398.0
Yungay pit 3	11.5±0.8	15.5±0.3	15672.4±190.0
TZ-0 pit 1	7.0±0.1	1.9±0.0	16.7±0.3
TZ-0 pit 2	4.1±0.1	1.4±0.0	25.7±0.4
TZ-0 pit 3	6.2±0.1	2.5±0.0	28.2±0.3
TZ-4 pit 1	3029.6±27.8	3002.3±26.8	165.9±2.2
TZ-4 pit 2	5040.2±48.6	7448.2±66.7	338.9±3.5
TZ-4 pit 3	2615.0±26.5	4456.0±43.6	1212.0±13.5
TZ-5 pit 1	38.2±0.4	3.0±0.1	13.7±0.1
TZ-5 pit 2	328.9±2.5	6.0±0.1	1606.4±10.7
TZ-5 pit 3	3132.1±19.9	20.9±0.2	3564.0±18.9
TZ-6 pit 1	113.9±0.8	11.7±0.2	95.9±0.8
TZ-6 pit 2	2981.5±18.5	140.6±1.3	1660.8±10.3
TZ-6 pit 3	1269.0±9.8	82.4±0.8	489.4±3.9

Table S3. Bacterial viability and abundance within AT-17 soil determined by trypan blue staining assay analyses.

Sample	log(viable cells/g)	log(non-viable cells/g)	log(total cells/g)	viable : non-viable (cells/cells)
MES	6.67	5.76	6.72	8.04
PONR	6.25	5.67	6.35	3.81
Yungay	6.32	5.78	6.43	3.48
TZ-0	6.77	5.99	6.84	6.07
TZ-4	6.53	6.43	6.78	1.24
TZ-5	6.26	6.39	6.66	0.73
TZ-6	6.70	6.37	6.90	2.15

Table S4. Colony forming units (CFUs) of AT-17 soil samples on ultrapure agarose, tryptic soy agar, LB agar, and plate count agar plates without amendments, amended with water, and amended with 10% sodium chloride, 10% sodium sulfate, 10% sodium carbonate, 10% sodium acetate, and 10% sodium L-lactate.

Type of culture plate	Amendment	MES	PONR	Yungay	TZ-0	TZ-4	TZ-5	TZ-6
Ultrapure agarose	None	15	186	55	770	5.73×10^3	968	5.29×10^3
	1.5 mL H_2O	0	207	196	100	2.71×10^3	69	437

	3 mL H_2O	0	481	134	195	3.07×10^3	104	1.25×10^3
	4.5 mL H_2O	0	15	106	111	3.57×10^3	87	667
	Chloride	0	2	459	295	3248	4.09×10^3	2.90×10^3
	Sulfate	0	0	2	27	1595	87	773
	Carbonate	0	5	104	0	1175	87	3.50×10^3
	Acetate	0	0	247	488	406	696	1.51×10^3
	L-lactate	218	1.08×10^3	503	1.12×10^3	116	3.68×10^3	1.02×10^3
Tryptic soy agar	None	37	53	169	514	1.60×10^5	1.33×10^5	3.21×10^5
	1.5 mL H_2O	523	140	44	297	1.09×10^5	5.75×10^4	2.21×10^5
	3 mL H_2O	41	35	6.29×10^3	288	8.00×10^4	1.20×10^5	4.29×10^5
	4.5 mL H_2O	5.76×10^3	3.39×10^3	1.14×10^4	312	1.65×10^6	5.22×10^4	5.09×10^5
	Chloride	7	12	3.6×10^4	181	4.21×10^4	8.70×10^5	5.26×10^5
	Sulfate	22	5	1.28×10^4	1.18×10^3	2.80×10^5	3.47×10^5	5.16×10^5
	Carbonate	394	10	2.69×10^4	7	298	5.44×10^4	3.68×10^5
	Acetate	2	2	92	268	5.08×10^5	1.45×10^5	1.11×10^6
	L-lactate	2.19×10^4	58	6.94×10^3	575	1.77×10^6	8.34×10^4	4.77×10^5
LB agar	None	17	28	33	91	2.39×10^5	2.95×10^3	5.41×10^4
	1.5 mL H_2O	71	54	13	140	8.18×10^3	1.81×10^3	1.65×10^5
	3 mL H_2O	37	93	7.51×10^3	241	2.67×10^4	4.93×10^3	1.14×10^5
	4.5 mL H_2O	7	7.98×10^3	3.71×10^3	491	1.23×10^6	1.17×10^3	1.54×10^5
	Chloride	0	2	219	135	3.03×10^3	986	1.19×10^5
	Sulfate	22	2	145	858	9.37×10^3	2.96×10^3	3.71×10^5
	Carbonate	2.68×10^3	15	53	0	305	1.96×10^3	4.49×10^3
	Acetate	10	5	243	358	5.44×10^5	4.35×10^3	6.01×10^5
	L-lactate	162	184	1.10×10^4	1.08×10^3	3.28×10^6	6.21×10^3	4.27×10^5
Plate count agar	None	167	190	8.06×10^3	1.40×10^3	6.89×10^6	1.82×10^4	1.25×10^6
	1.5 mL H_2O	744	8.43×10^3	8.43×10^3	311	3.22×10^6	5.87×10^4	6.44×10^6
	3 mL H_2O	2.09×10^3	254	4.55×10^4	243	2.67×10^6	2.60×10^4	5.93×10^5
	4.5 mL H_2O	1.36×10^3	8.56×10^4	6.96×10^4	638	1.33×10^7	1.25×10^5	4.12×10^6
	Chloride	2	53	29	237	1.89×10^6	5.80×10^4	5.68×10^5
	Sulfate	94	880	0	9.18×10^3	6.09×10^6	5.80×10^4	4.18×10^5
	Carbonate	1.61×10^3	176	174	53	4.35×10^3	6.38×10^4	1.74×10^5
	Acetate	2	19	135	193	2.67×10^6	2.32×10^4	1.33×10^6
	L-lactate	2.93×10^3	297	6.82×10^4	2.84×10^3	2.78×10^7	3.97×10^5	2.60×10^6

References

1. Hartley, A.J.; Chong, G.; Houston, J.; Mather, A.E. 150 million years of climatic stability: evidence from the Atacama Desert, northern Chile. *J Geol Soc London* **2005**, *162*, 421-424, doi:10.1144/0016-764904-071.
2. Navarro-Gonzalez, R.; Rainey, F.A.; Molina, P.; Bagaley, D.R.; Hollen, B.J.; de la Rosa, J.; Small, A.M.; Quinn, R.C.; Grunthaner, F.J.; Caceres, L., et al. Mars-like soils in the Atacama Desert, Chile, and the dry limit of microbial life. *Science* **2003**, *302*, 1018-1021, doi:10.1126/science.1089143.
3. Contador, C.A.; Veas-Castillo, L.; Tapia, E.; Antipan, M.; Miranda, N.; Ruiz-Tagle, B.; Garcia-Araya, J.; Andrews, B.A.; Marin, M.; Dorador, C., et al. Atacama Database: a platform of the microbiome of the Atacama Desert. *Antonie Van Leeuwenhoek* **2019**, 10.1007/s10482-019-01328-x, doi:10.1007/s10482-019-01328-x.
4. Schulze-Makuch, D.; Wagner, D.; Kounaves, S.P.; Mangelsdorf, K.; Devine, K.G.; de Vera, J.P.; Schmitt-Kopplin, P.; Grossart, H.P.; Parro, V.; Kaupenjohann, M., et al. Transitory microbial habitat in the hyperarid Atacama Desert. *P Natl Acad Sci USA* **2018**, *115*, 2670-2675, doi:10.1073/pnas.1714341115.

5. Cockell, C.S.; Brown, S.; Landenmark, H.; Samuels, T.; Siddall, R.; Wadsworth, J. Liquid Water Restricts Habitability in Extreme Deserts. *Astrobiology* **2017**, *17*, 309-318, doi:10.1089/ast.2016.1580.
6. Azua-Bustos, A.; Fairen, A.G.; Gonzalez-Silva, C.; Ascaso, C.; Carrizo, D.; Fernandez-Martinez, M.A.; Fernandez-Sampedro, M.; Garcia-Descalzo, L.; Garcia-Villadangos, M.; Martin-Redondo, M.P., et al. Unprecedented rains decimate surface microbial communities in the hyperarid core of the Atacama Desert. *Sci Rep-Uk* **2018**, *8*, 16706, doi:10.1038/s41598-018-35051-w.
7. Stevenson, A.; Burkhardt, J.; Cockell, C.S.; Cray, J.A.; Dijksterhuis, J.; Fox-Powell, M.; Kee, T.P.; Kminek, G.; McGenity, T.J.; Timmis, K.N., et al. Multiplication of microbes below 0.690 water activity: implications for terrestrial and extraterrestrial life. *Environ Microbiol* **2015**, *17*, 257-277, doi:10.1111/1462-2920.12598.
8. Armstrong, A.; Valverde, A.; Ramond, J.B.; Makhalanyane, T.P.; Jansson, J.K.; Hopkins, D.W.; Aspray, T.J.; Seely, M.; Trindade, M.I.; Cowan, D.A. Temporal dynamics of hot desert microbial communities reveal structural and functional responses to water input. *Sci Rep-Uk* **2016**, *6*, 34434, doi:10.1038/srep34434.
9. Uritskiy, G.; Getsin, S.; Munn, A.; Gomez-Silva, B.; Davila, A.; Glass, B.; Taylor, J.; DiRuggiero, J. Halophilic microbial community compositional shift after a rare rainfall in the Atacama Desert. *Isme J* **2019**, *13*, 2737–2749, doi:10.1038/s41396-019-0468-y.
10. Fernandez-Martinez, M.A.; Severino, R.D.; Moreno-Paz, M.; Gallardo-Carreno, I.; Blanco, Y.; Warren-Rhodes, K.; Garcia-Villadangos, M.; Ruiz-Bermejo, M.; Barberan, A.; Wettergreen, D., et al. Prokaryotic Community Structure and Metabolisms in Shallow Subsurface of Atacama Desert Playas and Alluvial Fans After Heavy Rains: Repairing and Preparing for Next Dry Period. *Front Microbiol* **2019**, *10*, 1641, doi:10.3389/fmicb.2019.01641.
11. Ramirez, R.M.; Craddock, R.A. The geological and climatological case for a warmer and wetter early Mars. *Nat Geosci* **2018**, *11*, 230-237, doi:10.1038/s41561-018-0093-9.
12. Martinez, G.M.; Renno, N.O. Water and Brines on Mars: Current Evidence and Implications for MSL. *Space Sci Rev* **2013**, *175*, 29-51, doi:10.1007/s11214-012-9956-3.
13. Azua-Bustos, A.; Caro-Lara, L.; Vicuna, R. Discovery and microbial content of the driest site of the hyperarid Atacama Desert, Chile. *Env Microbiol Rep* **2015**, *7*, 388-394, doi:10.1111/1758-2229.12261.
14. Makhalanyane, T.P.; Valverde, A.; Gunnigle, E.; Frossard, A.; Ramond, J.B.; Cowan, D.A. Microbial ecology of hot desert edaphic systems. *FEMS Microbiol Rev* **2015**, *39*, 203-221, doi:10.1093/femsre/fuu011.
15. McKay, C.P.; Friedmann, E.I.; Gomez-Silva, B.; Caceres-Villanueva, L.; Andersen, D.T.; Landheim, R. Temperature and moisture conditions for life in the extreme arid region of the Atacama Desert: Four years of observations including the El Nino of 1997-1998. *Astrobiology* **2003**, *3*, 393-406, doi:10.1089/153110703769016460.
16. Brocks, J.J.; Banfield, J. Unravelling ancient microbial history with community proteogenomics and lipid geochemistry. *Nat Rev Microbiol* **2009**, *7*, 601-609, doi:10.1038/nrmicro2167.
17. Shen, J.; Zerkle, A.L.; Stueken, E.E.; Claire, M.W. Nitrates as a Potential N Supply for Microbial Ecosystems in a Hyperarid Mars Analog System. *Life* **2019**, *9*, 79, doi:10.3390/life9040079.
18. Bagaley, D.R. Uncovering bacterial diversity on and below the surface of a hyper-arid environment, the Atacama Desert, Chile. Louisiana State University and Agricultural and Mechanical College, 2006.
19. Ericksen, G.E. The Chilean Nitrate Deposits. *Am Sci* **1983**, *71*, 366-374.
20. Shirey, T.B. Investigating microbial communities and the environmental factors influencing them in manmade and naturally occurring systems. University of Alabama, Tuscaloosa, Alabama, 2013.
21. Pruett, C.J.H.; Burges, H.D.; Wyborn, C.H. Effect of Exposure to Soil on Potency and Spore Viability of Bacillus-Thuringiensis. *J Invertebr Pathol* **1980**, *35*, 168-174, doi:10.1016/0022-2011(80)90179-2.
22. Artz, R.R.E.; Townend, J.; Brown, K.; Towers, W.; Killham, K. Soil macropores and compaction control the leaching potential of Escherichia coli O157 : H7. *Environ Microbiol* **2005**, *7*, 241-248, doi:10.1111/j.1462-2920.2004.00690.x.
23. Hansen, A.A.; Herbert, R.A.; Mikkelsen, K.; Jensen, L.L.; Kristoffersen, T.; Tiedje, J.M.; Lomstein, B.A.; Finster, K.W. Viability, diversity and composition of the bacterial community in a high Arctic permafrost soil from Spitsbergen, Northern Norway. *Environ Microbiol* **2007**, *9*, 2870-2884, doi:10.1111/j.1462-2920.2007.01403.x.
24. Saul-Tcherkas, V.; Steinberger, Y. Soil Microbial Diversity in the Vicinity of a Negev Desert Shrub-Reaumuria negevensis. *Microb Ecol* **2011**, *61*, 64-81, doi:10.1007/s00248-010-9763-x.
25. Shi, T.; Reeves, R.H.; Gilichinsky, D.A.; Friedmann, E.I. Characterization of viable bacteria from Siberian permafrost by 16S rDNA sequencing. *Microb Ecol* **1997**, *33*, 169-179, doi:10.1007/s002489900019.
26. Janssen, P.H.; Yates, P.S.; Grinton, B.E.; Taylor, P.M.; Sait, M. Improved culturability of soil bacteria and isolation in pure culture of novel members of the divisions Acidobacteria, Actinobacteria, Proteobacteria, and Verrucomicrobia. *Appl Environ Microb* **2002**, *68*, 2391-2396, doi:10.1128/Aem.68.5.2391-2396.2002.

27. Parinkina, O. Determination of bacterial growth rates in tundra soils. *Bulletins from the Ecological Research Committee* **1973**, 303-309.
28. Ma, R.P.; Xu, J.Y.; Wang, W.B.; Yuan, W. Seasonal and latitudinal differences of the saturation effect between ionospheric NmF2 and solar activity indices. *J Geophys Res-Space* **2009**, *114*, doi:10.1029/2009ja014353.
29. Warren-Rhodes, K.A.; Lee, K.C.; Archer, S.D.J.; Cabrol, N.; Ng-Boyle, L.; Wettergreen, D.; Zacny, K.; Pointing, S.B.; Chong, G.; Demargasso, C., et al. Subsurface Microbial Habitats in an Extreme Desert Mars-Analog Environment. *Front Microbiol* **2019**, *10*, 69, doi:10.3389/fmicb.2019.00069.
30. Zahran, H.H. Diversity, adaptation and activity of the bacterial flora in saline environments. *Biol Fert Soils* **1997**, *25*, 211-223, doi:10.1007/s003740050306.
31. Gómez-Silva, B.; Rainey, F.A.; Warren-Rhodes, K.A.; McKay, C.P.; Navarro-González, R. Atacama Desert soil microbiology. In *Microbiology of extreme soils*, Springer: Berlin, Heidelberg, 2008; pp. 117-132.
32. Lester, E.D.; Satomi, M.; Ponce, A. Microflora of extreme arid Atacama Desert soils. *Soil Biol Biochem* **2007**, *39*, 704-708, doi:10.1016/j.soilbio.2006.09.020.
33. Davis, W.L.; de Pater, I.; McKay, C.P. Rain infiltration and crust formation in the extreme arid zone of the Atacama Desert, Chile. *Planet Space Sci* **2010**, *58*, 616-622, doi:10.1016/j.pss.2009.08.011.
34. Marion, G.M.; Verburg, P.S.J.; McDonald, E.V.; Arnone, J.A. Modeling salt movement through a Mojave Desert soil. *J Arid Environ* **2008**, *72*, 1012-1033, doi:10.1016/j.jaridenv.2007.12.005.
35. Quinn, R.C.; Ehrenfreund, P.; Grunthaner, F.J.; Taylor, C.L.; Zent, A.P. Decomposition of aqueous organic compounds in the Atacama Desert and in Martian soils. *J Geophys Res-Biogeo* **2007**, *112*, doi:10.1029/2006jg000312.
36. Azua-Bustos, A.; Gonzalez-Silva, C.; Arenas-Fajardo, C.; Vicuna, R. Extreme environments as potential drivers of convergent evolution by exaptation: the Atacama Desert Coastal Range case. *Front Microbiol* **2012**, *3*, doi:10.3389/fmicb.2012.00426.
37. Davila, A.F.; Gomez-Silva, B.; de los Rios, A.; Ascaso, C.; Olivares, H.; Mckay, C.P.; Wierzchos, J. Facilitation of endolithic microbial survival in the hyperarid core of the Atacama Desert by mineral deliquescence. *J Geophys Res-Biogeo* **2008**, *113*, doi:10.1029/2007jg000561.
38. Finstad, K.; Probst, A.J.; Thomas, B.C.; Andersen, G.L.; Demergasso, C.; Echeverria, A.; Amundson, R.G.; Banfield, J.F. Microbial Community Structure and the Persistence of Cyanobacterial Populations in Salt Crusts of the Hyperarid Atacama Desert from Genome-Resolved Metagenomics. *Front Microbiol* **2017**, *8*, 1435, doi:10.3389/fmicb.2017.01435.
39. Palacio, S.; Azorin, J.; Montserrat-Marti, G.; Ferrio, J.P. The crystallization water of gypsum rocks is a relevant water source for plants. *Nat Commun* **2014**, *5*, 4660, doi:10.1038/ncomms5660.
40. Shen, J.; Smith, A.C.; Claire, M.W.; Zerkle, A.L. Unraveling biogeochemical phosphorus dynamics in hyperarid Mars-analogue soils using stable oxygen isotopes in phosphate. *Geobiology* **2020**, *00*, 1-20, doi:10.1111/gbi.12408.
41. Korehi, H.; Blothe, M.; Sitnikova, M.A.; Dold, B.; Schippers, A. Metal mobilization by iron- and sulfur-oxidizing bacteria in a multiple extreme mine tailings in the Atacama Desert, Chile. *Environ Sci Technol* **2013**, *47*, 2189-2196, doi:10.1021/es304056n.
42. Stivaletta, N.; Barbieri, R.; Cevenini, F.; López-García, P. Physicochemical conditions and microbial diversity associated with the evaporite deposits in the Laguna de la Piedra (Salar de Atacama, Chile). *Geomicrobiol J* **2011**, *28*, 83-95, doi:10.1080/01490451003653102.
43. Harris, J.K.; Cousins, C.R.; Claire, M.W. Spectral identification and quantification of salts in the Atacama Desert. *Proc Spie* **2016**, *10005*, doi:10.1117/12.2241520.
44. Idris, H.; Goodfellow, M.; Sanderson, R.; Asenjo, J.A.; Bull, A.T. Actinobacterial Rare Biospheres and Dark Matter Revealed in Habitats of the Chilean Atacama Desert. *Sci Rep-Uk* **2017**, *7*, doi:10.1038/s41598-017-08937-4.
45. Rose, H.L.; Dewey, C.A.; Ely, M.S.; Willoughby, S.L.; Parsons, T.M.; Cox, V.; Spencer, P.M.; Weller, S.A. Comparison of Eight Methods for the Extraction of Bacillus atrophaeus Spore DNA from Eleven Common Interferents and a Common Swab. *Plos One* **2011**, *6*, doi:10.1371/journal.pone.0022668.
46. Omelchenko, M.V.; Wolf, Y.I.; Gaidamakova, E.K.; Matrosova, V.Y.; Vasilenko, A.; Zhai, M.; Daly, M.J.; Koonin, E.V.; Makarova, K.S. Comparative genomics of Thermus thermophilus and Deinococcus radiodurans: divergent routes of adaptation to thermophily and radiation resistance. *Bmc Evol Biol* **2005**, *5*, doi:10.1186/1471-2148-5-57.
47. Battista, J.R.; Earl, A.M.; Park, M.J. Why is Deinococcus radiodurans so resistant to ionizing radiation? *Trends Microbiol* **1999**, *7*, 362-365, doi:10.1016/S0966-842x(99)01566-8.